

Revisiting Kinematic Fast Dynamo in 3-dimensional magnetohydrodynamic plasmas: Dynamo transition from non-Helical to Helical flows

Shishir Biswas,^{1,2*} Rajaraman Ganesh,^{1,2†}

¹*Institute for Plasma Research, Bhat, Gandhinagar, Gujarat 382428, India*

²*Homi Bhabha National Institute, Training School Complex, Anushaktinagar, Mumbai 400094, India*

Accepted XXX. Received YYY; in original form ZZZ

ABSTRACT

Dynamos wherein magnetic field is produced from velocity fluctuations are fundamental to our understanding of several astrophysical and/or laboratory phenomena. Though fluid helicity is known to play a key role in the onset of dynamo action, its effect is yet to be fully understood. In this work, a fluid flow proposed recently [Yoshida et al. Phys. Rev. Lett. 119, 244501 (2017)] is invoked such that one may inject zero or finite fluid helicity using a control parameter, at the beginning of the simulation. Using a simple kinematic fast dynamo model, we demonstrate unambiguously the strong dependency of short scale dynamo on fluid helicity. In contrast to conventional understanding, it is shown that fluid helicity does strongly influence the physics of short scale dynamo. To corroborate our findings, late time magnetic field spectra for various values of injected fluid helicity is presented along with rigorous “geometric” signatures of the 3D magnetic field surfaces, which shows a transition from “untwisted” to “twisted” sheet to “cigar” like configurations. It is also shown that one of the most studied ABC dynamo model is not the “fastest” dynamo model for problems with lower magnetic Reynolds number. This work brings out, for the first time, the role of fluid helicity in moving from “non-dynamo” to “dynamo” regime systematically.

Key words: fluid simulation – plasmas – magnetohydrodynamics – dynamo – magnetic fields

1 INTRODUCTION

The theories of HydroDynamics (HD) (Kraichnan 1965; Brachet et al. 1988) and MagnetoHydroDynamics (MHD) (Biskamp 2003; Beresnyak 2019; Schekochihin 2022) are often used to analyze the HD turbulence and magnetized plasma turbulence respectively, which are fundamental to our understanding of the behaviour of astrophysical plasmas present in the Sun or other young stars. The presence of small scale, mean or large scale magnetic fields are very much common in such astrophysical objects, planets, stars, interstellar medium, galaxy, accretion disks and also in the Sun (Squire & Bhattacharjee 2014a,b, 2015). Understanding the origin of these multi scale magnetic fields, which are in turn responsible for various complex phenomenon in the universe, is of paramount importance. Naturally a relevant question arises as to, what are the sources of these multi scale magnetic energy? As first pointed out by Parker, such magnetic fields are generated by the motions of conducting fluids through a transfer of kinetic to magnetic energy, that is, via Dynamo action (Parker 1979).

Depending on the length scales involved, dynamos are broadly classified into two categories : Small Scale Dynamo (SSD) and Large Scale Dynamo (LSD) or mean field dynamo. For LSD, it is believed that a lack of reflectional symmetry (or in other words, nonzero fluid

helicity) to be a crucial element, whereas for SSD, no correlation has been shown to exist between onset and sustenance of SSD on fluid helicity (Rincon 2019). Depending on the time scale, dynamos may further divided into two categories: Fast dynamos (growth rate can remain finite in the limit $R_m \rightarrow \infty$) and Slow dynamos (magnetic diffusion plays a significant role) (Rincon 2019). Depending on the feedback strength of the magnetic field on to the fluid motion, dynamos are categorized as linear or non-linear. A linear dynamo is one in which the magnetic field dynamics does not “back react” with the velocity field and the velocity field is either given or it obeys the NS equation (Rincon 2019), whereas a self-consistent dynamo or a nonlinear dynamo tends to change the flow - as the magnetic field becomes large enough - to further impede magnetic field growth. That is, the flow and the B-field “back react” on each other leading to a nonlinear saturation (Rincon 2019).

In the present study, we focus on a kinematic fast dynamo model, wherein velocity and magnetic fields are un-correlated. As indicated earlier, in a fast dynamo model, below a certain value of resistivity, the growth rate becomes insensitive to the magnitude of resistivity, i.e, becomes independent of resistivity. (Childress & Gilbert 1995). A popular example of fast dynamo is the Solar dynamo (Choudhuri 1990).

It is now well acknowledged that, to achieve fast dynamo, an careful selection of plasma flow profile is necessary, as the key mechanism behind the fast dynamo action is that of stretching, twisting and folding (STF) of magnetic field lines, “advected” in the fluid flow.

* E-mail: shishirbeafriend@gmail.com, shishir.biswas@ipr.res.in

† E-mail: ganesh@ipr.res.in

Hence the flow is expected to have “enough dynamics” to amplify the magnetic field exponentially.

As discussed before, depending on the length scale involved, dynamos are largely classified into two broad categories : Small Scale Dynamo (SSD) and Large Scale Dynamo (LSD). For a LSD or mean field dynamo, a lack of reflectional symmetry is required, where as conventional understanding is that, no such condition is expected to be satisfied for SSD (Rincon 2019). Among various astrophysical flows addressed, the Arnold-Beltrami-Childress [ABC] flow is a well known prototype for fast dynamo action for its stretching ability and chaotic transport properties. A detailed dynamo study using ABC flow has been reported by various authors, eg. (Arnold & Korkina 1983; Galloway & Frisch 1984; Dombre et al. 1986; Galanti et al. 1992; Dorch 2000; Archontis, V. et al. 2003; Bouya & Dormy 2013). Along with the exponential growth of magnetic energy, the magnetic energy iso-surface are known to exhibit special signature called “cigar” like (Galloway & Frisch 1986) or “ribbon” like (Galloway & Frisch 1986; Archontis, V. et al. 2003) structure. For ABC flow profile, the vorticity field is parallel to the velocity direction, i.e. $\vec{\nabla} \times \vec{u}$ has a finite parallel component to \vec{u} at all times. This naturally indicates that, finite fluid helicity $[\int_V \vec{u} \cdot (\vec{\nabla} \times \vec{u}) dV]$ is present in the flow. The fluid helicity effect on dynamo action is often expressed as α effect, and studied extensively using ABC flow family (Courvoisier et al. 2006).

Study of dynamo instability using a 3D flows becomes numerically demanding and is perhaps relatively more complex. To reduce the complexity in numerical methods often, time dependent two dimensional flows $[\vec{u}(x, y, t)]$ have been taken into consideration for the investigation of fast dynamo action. Naturally, the presence of time dependency introduces chaoticity in such flows. Galloway-Proctor flow, sometimes known as GP flow, is one such well-known flow (Galloway & Proctor 1992). In light of the fact that the flow profile is entirely independent of one spatial coordinate, in this case the z-coordinate, it is conceivable to seek monochromatic solutions for the magnetic field of the form $\vec{B}(x, y, z, t) = \vec{B}(x, y, t)e^{ik_z z}$, so that the problem becomes two-dimensional for a given value of k_z . In past several authors (Cattaneo et al. 1995, 1996; Hughes et al. 1996; Rädler & Brandenburg 2003) have investigated the dynamo instability using Galloway-Proctor (GP) flow. Recently GP flow (Galloway & Proctor 1992) has been taken into consideration for studying large scale magnetic fields in the presence of velocity shear (Tobias & Cattaneo 2013).

Some of the interesting and relevant questions are: is the small-scale kinematic fast dynamo action possible only for chaotic ABC flow and time dependent GP flow? what is the exact role of fluid helicity in the context of small-scale fast dynamo action? Is there flow field using which one can systematically inject fluid helicity in the system and clearly demonstrate a non-dynamo to dynamo transition when the fluid flow transits from non-helical to helical flow? Does the fluid helicity affect short-scale dynamo action?

In past several authors examined the influence of the flow helicity in the context of kinematic fast dynamo action. For example, Hughes et al. (1996) show that the small scale, fast dynamo will always exist regardless of the flow helicity distribution using three different types of helicity distribution (non zero local and global helicity, non zero local helicity but zero global helicity, and zero local and global helicity). The flow considered by Hughes et al. (1996) is a time dependent 2-dimensional flow $[\vec{u}(x, y, t)]$ (Galloway & Proctor 1992). As previously mentioned, the induction equation for magnetic field supports a monochromatic solution of the form $\vec{B}(x, y, t) \times e^{ik_z z}$, for a given k_z value, the resulting problem for the magnetic field is two-dimensional. The most significant finding was that the helicity

distribution of the driving flow did not significantly affect the small-scale fast dynamo action (Hughes et al. 1996). Additionally, it was pointed out that as fluid helicity increases, the dynamo growth rate noticeably increases. However, these Authors quickly clarify that this is only coincidence (Hughes et al. 1996).

By keeping these earlier ideas in mind, we study the fast dynamo action using a newly proposed Yoshida-Morrison flow or YM flow (Yoshida & Morrison 2017) to investigate the role of helicity on SSD. It is important to indicate that the whole class of YM flow depends upon all three spatial coordinates i.e. $\vec{u}(x, y, z)$ similar to ABC flow. We have considered small homogeneous ambient initial magnetic field in all 3 directions as considered earlier by Galloway & Frisch (1984); Dorch (2000); Archontis, V. et al. (2003). Another interesting and useful aspect of YM flow is that, it is possible to inject finite fluid helicity $[\int_V \vec{u} \cdot (\vec{\nabla} \times \vec{u}) dV]$ in the system, by systematically varying certain physical parameter. More over this flow has a special property that, it establishes a topological bridge between quasi 2-dimensional class and 3-dimensional class of flows. Therefore, our present study focuses on various flows with varying kinetic energy, chaotic characteristics, and helicity on the onset and sustenance of SSD.

In the present work, we propose a new possible route that connects non-dynamo regime to dynamo regime via fluid helicity injection using Yoshida-Morrison (YM) flow as a prototype. Our numerical observation demonstrates that small scale dynamo is feasible for this type of initial condition. Our work shows unambiguously that fluid helicity does affect the dynamics of small-scale dynamos. This finding is in complete contrast to the earlier results (Hughes et al. 1996). Our findings systematically connect most of the previous works and brings in several new insights. To corroborate our findings, time dependent magnetic energy spectra, for various magnitudes of injected fluid helicity is calculated. We also show that, how a “cigar” like iso-surface, which is a signature of fast dynamo action, emerges naturally starting from a non-dynamo iso-surface. Our numerical investigation also suggests that, for lower magnetic Reynolds number (R_m) experiments, the regular ABC dynamo model is not the best dynamo model.

The organization of the paper is as follows. In Sec. 2 we present about the dynamic equations. About our numerical solver and simulation details are described in Sec. 3. The initial conditions, parameter details are shown in Sec. 4. Section 5 is dedicated to the simulation results on induction dynamo action that we obtained from our code and finally the summary and conclusions are listed in Sec. 6.

2 GOVERNING EQUATIONS

The governing equations to study Kinematic Fast dynamo action for the single fluid MHD plasma are as follows,

$$\frac{\partial \vec{B}}{\partial t} + \vec{\nabla} \cdot (\vec{u} \otimes \vec{B} - \vec{B} \otimes \vec{u}) = \frac{1}{R_m} \nabla^2 \vec{B} \quad (1)$$

$$\vec{\nabla} \cdot \vec{B} = 0 \quad (2)$$

where, \vec{u} , B and R_m represent the velocity, magnetic fields and magnetic Reynolds number respectively. We define Alfvén speed as, $V_A = \frac{u_0}{M_A}$, here M_A is the Alfvén Mach number of the plasma and u_0 is the maximum fluid speed. The initial magnetic field (B_0) is determined as from Alfvén speed as, $V_A \propto B_0$. Time is normalized as $t = t_0 \times t'$, $t_0 = \frac{L}{V_A}$. The symbol “ \otimes ” represents the dyadic between two vector quantities.

For solving the above set of equations at high enough grid resolution, one need a suitable scalable numerical solver.

3 SIMULATION DETAILS: GMHD3D SOLVER

In this Section, we discuss the details of the numerical solver along with the benchmarking of the solver carried out by us. In order to study the plasma dynamics governed by MHD equations described above, we have very recently upgraded an already existing well bench-marked single GPU MHD solver (Mukherjee 2019), developed in house at Institute For Plasma Research to multi-node, multi-card (multi-GPU) architecture for better performance (Biswas et al. 2022a). The newly upgraded GPU based magnetohydrodynamic solver [GMHD3D] is now capable of handling very large grid sizes. GMHD3D is a multi-node, multi-card, three dimensional (3D), weakly compressible, pseudo-spectral, visco-resistive magnetohydrodynamic solver (Biswas et al. 2022a). It uses pseudo-spectral technique to simulate the dynamics of 3D magnetohydrodynamic plasma in a cartesian box with periodic boundary condition. By this technique one calculates the spatial derivative to evaluate non-linear term in governing equations with a standard $\frac{2}{3}$ de-aliasing rule (Patterson & Orszag 1971). OpenACC FFT library [AccFFT library (Gholami et al. 2016)] is used to perform Fourier transform and Adams-bashforth time solver, for time integration. For 3D iso-surface visualization, an open source Python based data converter to VTK [Visualization Tool kit] by “PyEVTK” (Paulo-herrera 2021) is developed, which converts ASCII data to VTK binary format. After dumping the state data files to VTK, an open source visualization softwares, VisIt 3.1.2 (LLNL 2020) and Paraview (Kitware 2022) is used to visualize the data. As mentioned earlier, we have upgraded a well benchmarked single GPU solver to multi-node, multi-card (multi-GPU) architecture, for this present work, the new solver’s accuracy with the single GPU solver has been cross-checked and it is verified that the results match upto machine precision. Further few more benchmarking studies have been performed such as, the 3D induction dynamo effect by (Galloway & Frisch 1986; Dorch 2000; Archontis, V. et al. 2003), have been reproduced with ABC flow at grid resolution 64^3 (Details of these are not presented here.).

To study the induction dynamo action, an accurate selection of “drive” velocity field is imperative, which we discuss in the Section to follow.

4 INITIAL CONDITION

The study of dynamo action or more precisely kinematic fast dynamo action in the presence of chaotic 3D Arnold-Beltrami-Childress [ABC] flow has been explored by various authors (Galloway & Frisch 1984; Dombre et al. 1986; Galanti et al. 1992; Dorch 2000; Archontis, V. et al. 2003; Bouya & Dormy 2013). The velocity field for ABC flow is as follows:

$$\begin{aligned} u_x &= u_0 [A \sin(k_0 z) + C \cos(k_0 y)] \\ u_y &= u_0 [B \sin(k_0 x) + A \cos(k_0 z)] \\ u_z &= u_0 [C \sin(k_0 y) + B \cos(k_0 x)] \end{aligned} \quad (3)$$

Recently Yoshida et al. (Yoshida & Morrison 2017) proposed a new intermediate class of flow, that establishes a topological bridge between quasi-2D and 3D flow classes. The flow is formulated as follows:

$$\vec{u} = \alpha \times u_0 \times \vec{u}_+ + \beta \times u_0 \times \vec{u}_- \quad (4)$$

with

$$\vec{u}_+ = \begin{bmatrix} B \sin(k_0 y) - C \cos(k_0 z) \\ 0 \\ A \sin(k_0 x) \end{bmatrix} \quad (5)$$

and

$$\vec{u}_- = \begin{bmatrix} 0 \\ C \sin(k_0 z) - A \cos(k_0 x) \\ -B \cos(k_0 y) \end{bmatrix} \quad (6)$$

so that,

$$\begin{aligned} u_x &= \alpha u_0 [B \sin(k_0 y) - C \cos(k_0 z)] \\ u_y &= \beta u_0 [C \sin(k_0 z) - A \cos(k_0 x)] \\ u_z &= u_0 [\alpha A \sin(k_0 x) - \beta B \cos(k_0 y)] \end{aligned} \quad (7)$$

where k_0, α, β, A, B and C are arbitrary real constants. As indicated earlier, we dub this flow (Eq. 7) as Yoshida-Morrison flow or YM flow. We consider the value of k_0, α, A, B and C to be unity for this present study. The variation of β value in YM flow leads to new classes of flows.

For example, for $\beta = 0$, Yoshida et al. (Yoshida & Morrison 2017) classifies it as EPI-2D flow [See Fig. 1a] which is given by :

$$\begin{aligned} u_x &= u_0 [\sin(y) - \cos(z)] \\ u_y &= 0 \\ u_z &= u_0 [\sin(x)] \end{aligned} \quad (8)$$

This flow (i.e, Eq. 8) is dependent on all the 3 spatial coordinates (i.e, x, y, z), whereas only two flow components are nonzero. Thus EPI-2D flow is quasi-2D in nature.

As can be expected, for $\beta = 1$ the above Eq. 7 becomes well known ABC like flow [See Fig. 1f],

$$\begin{aligned} u_x &= u_0 [\sin(y) - \cos(z)] \\ u_y &= u_0 [\sin(z) - \cos(x)] \\ u_z &= u_0 [\sin(x) - \cos(y)] \end{aligned} \quad (9)$$

(The only mathematical difference between the flow described in Eq. 9 and the ABC flow [Eq. 3] are that the two terms are being subtracted in the latter while added in the former. Nevertheless, as will be shown below, the flow in Eq. 9 is identical in its properties to ABC flow [Eq. 3].) As β is varied from 0 to 1.0, a whole set of intermediate class of flows emerge, such that a normalized fluid helicity is exactly 0.0 for $\beta = 0$ and is maximum for $\beta = 1.0$ (i.e, ABC-like flows). For a comprehensive study, we explore various values of β between 0 to 1, keeping all other parameters identical [See Fig. 1b, 1c, 1d, 1e].

By increasing β values we inject normalized fluid helicity in the system [See. Appendix A for details]. In Fig. 2, normalized fluid helicity $[\int_V \vec{u} \cdot (\vec{\nabla} \times \vec{u}) dV]$ is calculated, for YM flow. It is observed that for increasing β values normalized fluid helicity also increases. It is also interesting to note from YM flow velocity contour visualization [See Fig. 1a, 1b, 1c, 1d, 1e, 1f] that for increasing β values, the velocity contours become increasingly chaotic and visible separatrix forms emerge, which is a crucial ingredient of chaotic flows. The maximum fluid velocity is $u_0 = 1.0$ and Alfvén Mach number is $M_A = 10.0$. Following (Galloway & Frisch 1984), the initial magnetic field is considered as very small but uniform in nature. With these given velocity fields, we perform our simulation, the details of which is given next.

4.1 Parameter Details

We evolve the above set of equations discussed in Section 2, for class of YM flow profile, in a triply periodic box of length $L_x = L_y = L_z = 2\pi$ with time stepping (dt) = 10^{-4} and grid resolution 256^3 . We have performed grid size scaling study [See. Appendix B] using

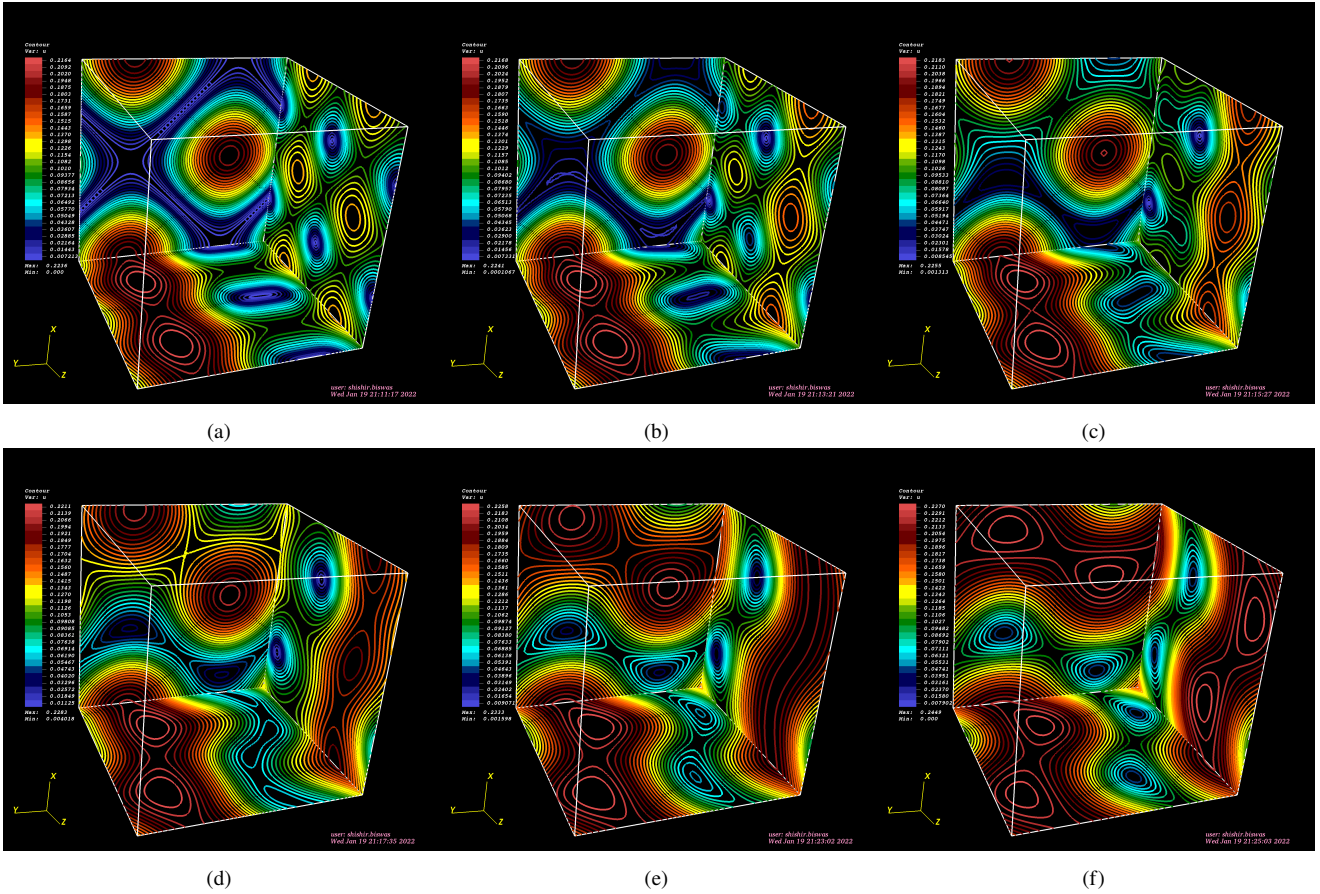


Figure 1. Driving velocity contours of Yoshida-Morrison (YM) flow. The velocity contour visualization is shown for (a) $\beta = 0.0$, (b) $\beta = 0.2$, (c) $\beta = 0.4$, (d) $\beta = 0.6$, (e) $\beta = 0.8$, (f) $\beta = 1.0$, where $\beta = 0.0$ is least chaotic and $\beta = 1.0$ is most chaotic. It is important to identify that for the increasing β values the velocity field lines are becoming chaotic and finally the visible separatrix has been formed for most helical (i.e. $\beta = 1.0$) case.

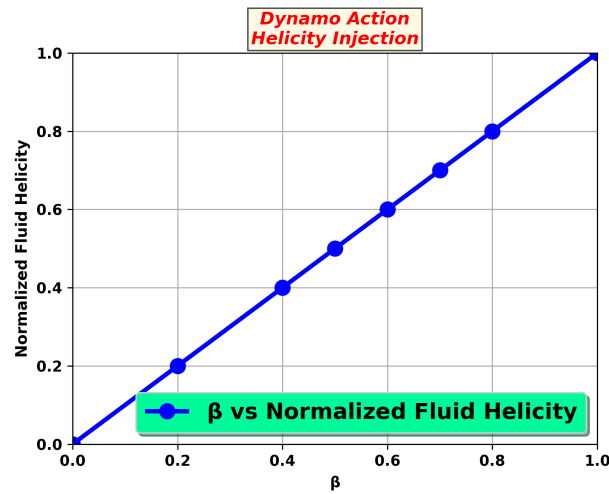


Figure 2. Normalized fluid helicity as a function of β for Yoshida-Morrison (YM) flow. Here β is real constant. $\beta = 0.0$ corresponds to non-helical (zero normalized fluid helicity) flow and $\beta = 1.0$ corresponds to maximum helical (maximum normalized fluid helicity) flow. For detail calculation and normalization [See. Appendix A].

Arnold-Beltrami-Childress (ABC) flow (Galloway & Frisch 1984) for different magnetic Reynolds numbers. It is obvious that 256^3 grid resolution is more than enough for this problem [See. Appendix B]. With these initial conditions and parameter spaces we present our numerical simulation results.

5 SIMULATION RESULTS

We consider a recently proposed general class of flow named YM flow (Eq. 7) (Yoshida & Morrison 2017) for this present study, as indicated earlier and evolve the homogeneous initial B-field in time, using Eq. 1 for a given set of values of β and u_0 using our GPU solver *GMHD3D*. An interesting and useful aspect of YM flow is that, it is possible to inject finite fluid helicity $[\int_V \vec{u} \cdot (\vec{\nabla} \times \vec{u}) dV]$ in the system [See Fig. 2], by systematically varying certain physically meaningful parameter, i.e. β .

We study the kinematic fast dynamo action for various β value starting from 0.0 to 1.0. For $\beta = 0.0$ value, YM flow leads to EPI-2 dimensional flow (Yoshida & Morrison 2017). EPI-2 dimensional flow makes a topological bridge between quasi-2D and 3D class of flows (Yoshida & Morrison 2017). We perform numerical runs for a wide range of magnetic Reynolds numbers (R_m). From Fig. 3a it is observed that, for $\beta = 0.0$ there is no prominent dynamo action, even at highest magnetic Reynolds numbers ($R_m = 5000$). At late times, magnetic energy curve is flat with respect to time, indicating that the growth rate is zero. The key mechanism behind the fast dynamo action is believed to be stretching, twisting and folding (STF) of magnetic field lines (Vainshtein & Zel'dovich 1972), that generates exponential growth of magnetic energy and hence it is necessary that, the flow should be able to “twist” (i.e., should contain enough chaoticity) and hence should contain nonzero fluid helicity to generate exponential growth of magnetic energy. From our earlier discussion it is already evident that, YM flow with $\beta = 0.0$ has zero fluid helicity and hence is not able to amplify the magnetic field in exponential manner i.e, not able to generate dynamo action.

It is important to note that, there are examples of non-helical flows, that can produce fast dynamo action, that is due to Cross-helicity effect or the so-called Yoshizawa effect (Galloway & Proctor 1992; Sur & Brandenburg 2009). Also as discussed in the Introduction, several authors have reported dynamo action using 2-dimensional time dependent non-helical flows. For example, GP flow (Galloway & Proctor 1992; Hughes et al. 1996), has been used to study kinematic fast dynamo action. The flow profile goes as $\vec{u}(x, y, t)$, so the initial magnetic field is modeled as $B(x, y, t) \times e^{ik_z z}$, for a fixed k_z , the resulting problem for the magnetic field is two-dimensional. Using these initial condition fast dynamo action has been reported for non-helical flows.

Let us come back to YM flow with β as the control parameter for initial helicity injected. We study of magnetic energy iso-surfaces for the $\beta = 0.0$ case and observe that most of the energy is concentrated in elongated almost two-dimensional un-twisted structures [See Fig. 3b]. To obtain better visualization, we also provide volume rendered view [See Fig. 3c] of magnetic energy iso-surfaces and pseudo-color view [See Fig. 3d] of magnetic energy iso-surfaces. These several visualizations (iso-surface view, volume rendering view, and pseudo-color view) aid in understanding the nature of iso-surfaces. Such magnetic structures have been reported earlier for kinematic dynamo simulations by Alexakis (2011) and are referred to as “magnetic ribbons”. It is clear that the structures do not have any twisting, which is due to the absence of fluid helicity in the flow field.

It was discussed earlier that, the injection of normalized fluid he-

licity in the system is possible by systematically varying some meaningful physical parameter, i.e. β value for YM flow. In the following, we perform numerical runs and present simulation results with $\beta = 0.2$ for various magnetic Reynolds numbers (R_m). The stretching, twisting and folding (STF) of magnetic field lines (Vainshtein & Zel'dovich 1972) doubles the magnetic field per cycle because of flux freezing. Presence of higher diffusivity in the system makes the flux freezing condition to be violated, which in turns results in, suppression of exponential growth of magnetic energy. Hence, the fast dynamo action gets hindered for a higher diffusive system. From Fig. 4a it is observed that, the YM flow ($\beta = 0.2$) efficiently amplifies the magnetic field in exponential manner for a wide range of R_m value and exhibits dynamo action. A careful observation of magnetic energy iso-surface shows that, the energy is concentrated in long and flat structures or “ribbon” like structures [See Fig. 4b, 4c, 4d]. Although small scale structures are also present here, they appear to be more “organized” to form special geometric patterns, which is reported earlier (Alexakis 2011). It is notable that, there is visible twisting in the “ribbons” that indicates the presence of fluid helicity in the flow. With respect to earlier case, it is identified that by varying β value from 0 to 0.2 we are able to produce fast dynamo action efficiently. For $\beta = 0.2$, there is fluid helicity present in the system and the presence of fluid helicity twists the ribbon which produces dynamo action.

To study the effect of fluid helicity in the context of kinematic fast dynamo action in detail, we explore various β values such as 0.4, 0.6, 0.8 and 1.0. For $\beta = 0.4$, we observe that the generation of exponential magnetic energy growth is possible for a substantial range of magnetic Reynolds number (R_m) [See Fig. 5a]. Due to the presence of finite fluid helicity in the system, the flow is able to produce dynamo action. From the magnetic energy iso-surface visualization, energy is seen to be concentrated in elongated structures [See Fig. 5b, 5c, 5d]. These structures are part of sheetlike structures reported earlier (Alexakis 2011), much like the “ribbons” [See Fig. 5b, 5c, 5d] observed for earlier cases as well.

For further higher β value say $\beta = 0.6$, it is observed that magnetic energy grows exponentially with time for a wide range of R_m values. We provide the results for magnetic Reynolds number (R_m) 50 to 5000 in small steps and observe that, for all the sets of numerical runs, there is prominent dynamo action [See Fig. 6a]. This is due to the presence of fluid helicity and twisting ability in the system. As in the earlier cases, the presence of fluid helicity promotes the twisting ability of the flow and that results in dynamo action. The magnetic energy is seen to concentrate in elongated sheetlike or “ribbon” like structures [See Fig. 6b, 6c, 6d] reported earlier as well (Alexakis 2011). The magnetic energy iso-surfaces form couple structures for some particular time. These structures are also seen similar to the “double ribbon” structures similar to the “double cigar” structures, reported earlier for ABC flow (Dorch 2000). In the simulation within the oscillatory regime, as the energy increases at the beginning of a ‘cycle’, the secondary ribbon increases in size until the two ribbon become equal in size and strength midway through the cycle [See Fig. 6b, 6c, 6d]. The primary ribbon now becomes smaller and actually vanishes at the end of the cycle, at which time the growth of the energy slows down. Towards the end of a cycle, the primary ribbon begins to decay, because the supply of flux to the primary ribbon is less than that to the secondary ribbon. At the end of one cycle the secondary ribbon is the only remaining structure.

Finally, we explore the only left β value, i.e. $\beta = 1.0$. As discussed earlier, YM flow with $\beta = 1.0$ regenerates the classical Arnold-Beltrami-Childress [ABC] flow. As in the earlier cases (viz. $\beta = 0.0, 0.2, 0.4, 0.8$), we provide runs for a wide range of magnetic

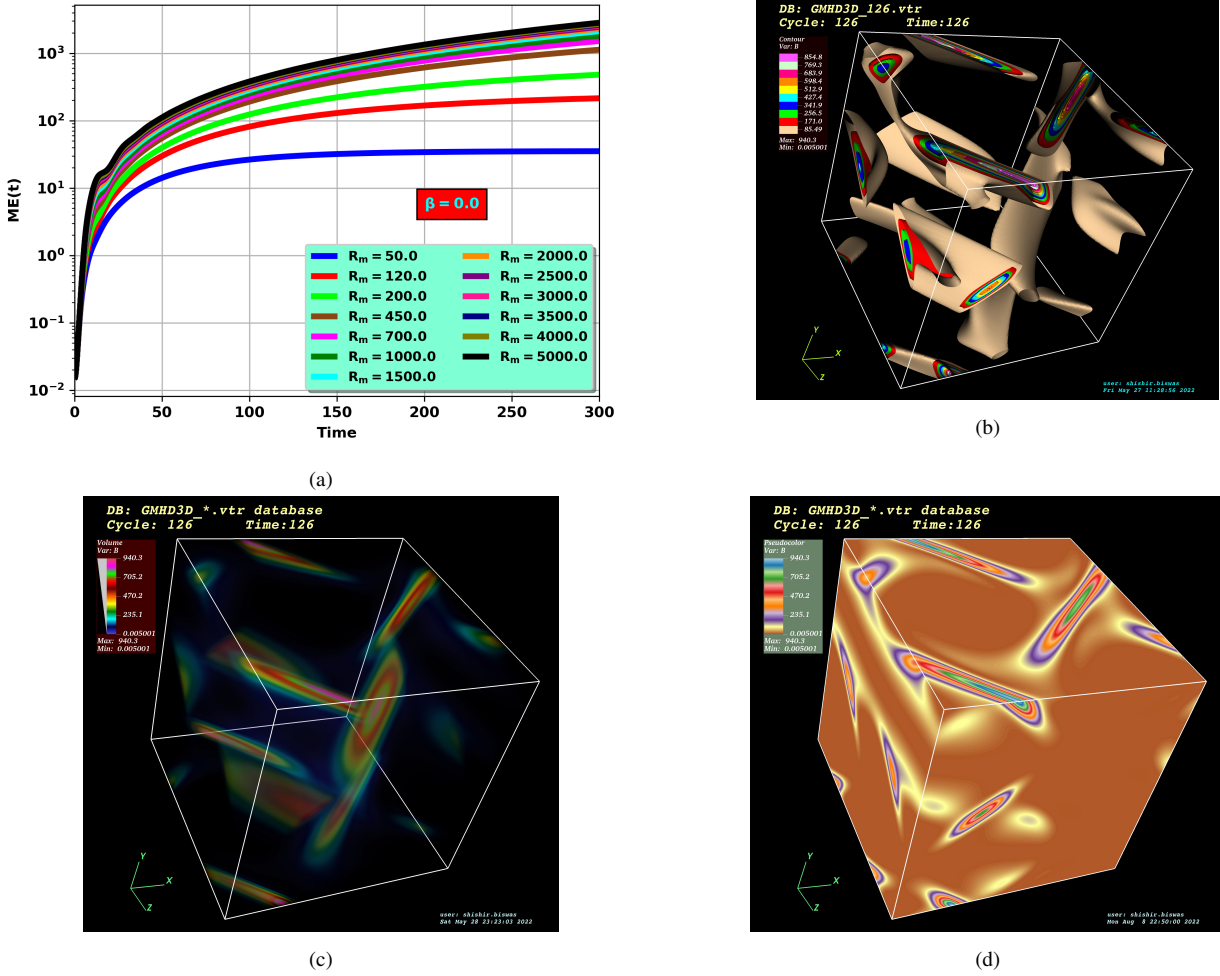


Figure 3. Kinematic fast Dynamo effect for different magnetic Reynolds number (R_m) using Yoshida-Morrison (YM) flow with $\beta = 0.0$. (a) The magnetic energy $\left(\int \frac{B^2(x,y,z,t)}{2} dV\right)$ growth is seen to be unaffected with increase of R_m . The (b) three-dimensional (3D) magnetic energy iso-surface [Supplementary movie added], (c) three-dimensional (3D) volume rendering view of magnetic energy iso-surfaces and (d) three-dimensional (3D) pseudo-color view of magnetic energy iso-surfaces (for magnetic Reynolds number $R_m = 50$) is seen identical as a untwisted “magnetic ribbon”. Simulation details: grid resolution 256^3 , stepping time $dt = 10^{-4}$, magnitude of fluid velocity $u_0 = 1.0$, Alfven mach number $M_A = 10.0$.

Reynolds number (R_m) starting from $R_m = 50$. As is expected, for $\beta = 1$, for all the sets of numerical runs, we observe significant magnetic energy growth [See Fig. 7a]. The visualization of this maximum helical ($\beta = 1.0$) flow leads to visible separatrix formation [See Fig. 1f], a signature of chaotic flow which drives the exponential energy growth for $\beta = 1.0$, as the flow becomes maximum helical similar like ABC flow. This exponential growth of magnetic energy using ABC flow via kinematic fast dynamo action is well explored so far by various authors (Galloway & Frisch 1986; Dorch 2000; Archontis, V. et al. 2003; Bouya & Dormy 2013). Probably the ABC flow is the most explored flow, that has been used for dynamo action. We also produce identical magnetic energy growth like ABC flow starting from an initial negligible value, using YM flow with $\beta = 1$ [See Fig. 7a]. The study of magnetic energy iso-surface also leads to an interesting observation. It is observed that, the exponentially growing nature of magnetic energy generates rigorous geometric structures or likely to say “cigar like” structures [See Fig. 7b, 7c, 7d], and it supported by literatures (Galloway & Frisch 1986; Dorch 2000; Archontis, V. et al. 2003; Bouya & Dormy 2013). From our numerical

experiments, we confirm that “cigar like” structure is a stable structure and its appearance is a signature for the onset of exponential growth in magnetic energy. Strong localization of the current density structures co-existing with magnetic “cigars”, due to magnetic reconnection, is also observed [See Fig. 7e].

By systematically varying the helicity parameter β in the YM flow (Yoshida & Morrison 2017) or in the other words by injecting normalized fluid helicity in the system, we have explored a systematic route that connects flat “ribbon” like structures to “twisted ribbon” and finally towards classical “cigar” like structures. The emergence of these significant structures (“ribbon”, “twisted ribbon”, “cigar”) due to the injected normalized fluid helicity are demonstrated via direct numerical simulation. Interestingly, though all these structures have been reported earlier, but the significant connection between these structures using a single fluid flow model, not explored so far. Here in this present study we connect all these different well known structures via normalized fluid helicity injection using YM flows.

Coming back to $\beta = 1.0$ case, as discussed, this class of flow is identical to the well known Arnold-Beltrami-Childress [ABC] flow.

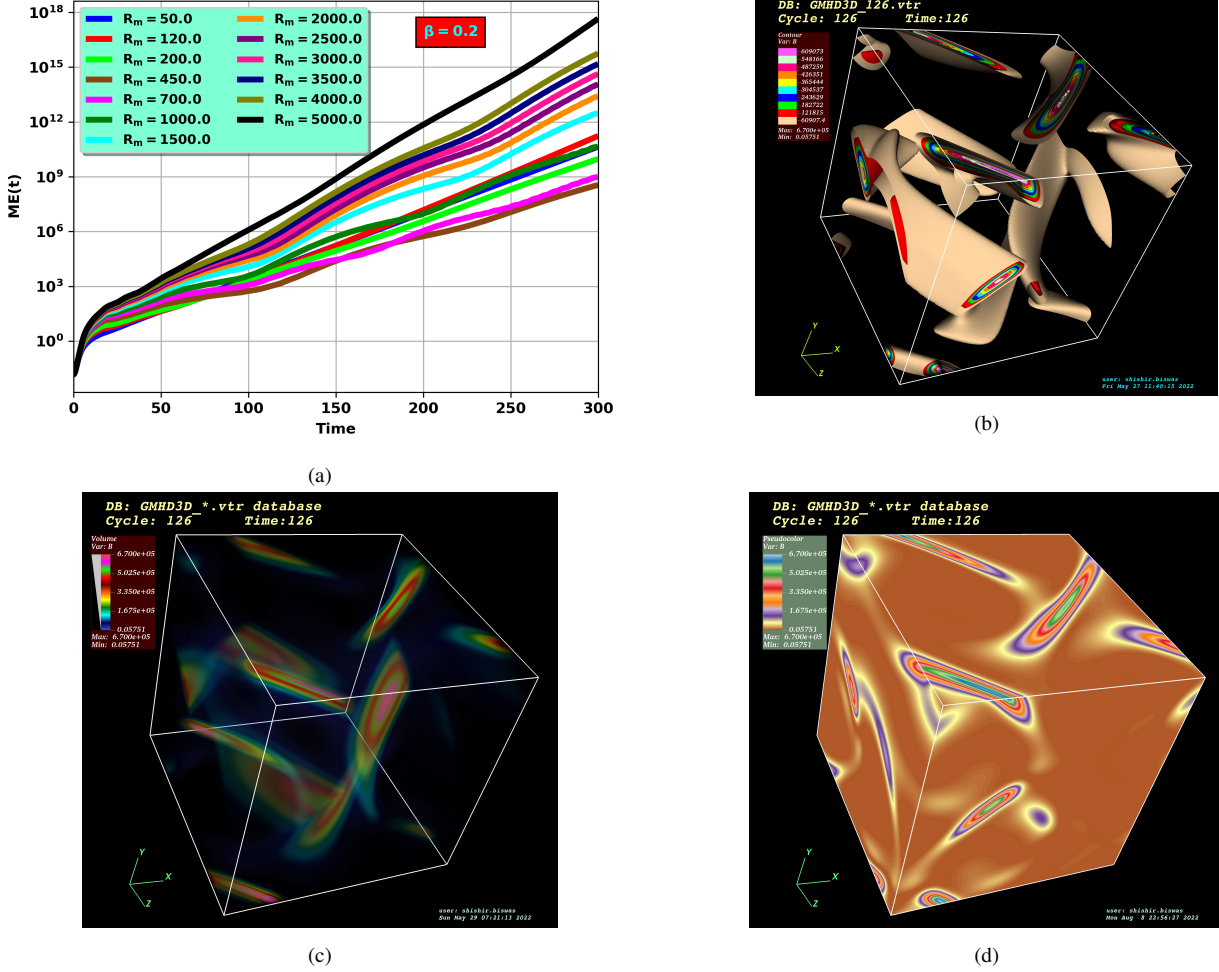


Figure 4. Kinematic fast Dynamo effect for different magnetic Reynolds number (R_m) using Yoshida-Morrison (YM) flow with $\beta = 0.2$. (a) The magnetic energy $\left(\sum \frac{B^2(x, y, z, t)}{2}\right)$ growth is observed for different R_m values. The (b) three-dimensional (3D) magnetic energy iso-surface [Supplementary movie added], (c) three-dimensional (3D) volume rendering view of magnetic energy iso-surfaces and (d) three-dimensional (3D) pseudo-color view of magnetic energy iso-surfaces (for magnetic Reynolds number $R_m = 50$) is seen to be twisted “ribbon” like nature. Note that the twisting indicates the presence of fluid helicity in the flow. Simulation details: grid resolution 256^3 , stepping time $dt = 10^{-4}$, magnitude of fluid velocity $u_0 = 1.0$, Alfvén mach number $M_A = 10.0$.

It is shown that, the fastest magnetic energy growth or the exponential energy growth for this kind of flow is signified by generation of a special kind of structure called “cigar” like structure. We study the magnetic Reynolds number (R_m) effect on the “cigar” structure. Keeping all the parameters identical, we perform numerical runs for various magnetic Reynolds number (R_m) and visualize the magnetic energy iso-surfaces [See Fig. 8a, 8b, 8c]. From figures 8a, 8b and 8c it is identified that, the thickness of a “cigar” (δ) decreases with the increase of magnetic Reynolds number (R_m). We also calculate the “cigar” thickness (δ) for various intermediate R_m and plot it [See Fig. 8d]. From Fig. 8d it is observed that, the “cigar” thickness (δ) decreases with R_m with a strong scaling of $\frac{1}{\sqrt{R_m}}$. This $\frac{1}{\sqrt{R_m}}$ scaling is also identified by various authors (Galloway & Frisch 1986; Archontis, V. et al. 2003) for ABC flow and suggests Sweet-Parker scaling. Here in this present study, we observe the identical scaling for YM flow ($\beta = 1$). As the change of magnetic Reynolds number (R_m) only changes the cigar thickness (δ), hence to help visualize, we plot iso-surfaces for magnetic Reynolds number ($R_m = 50$) for all the case discussed above.

We also calculate the magnetic energy growth rate for all β cases. It is seen from Fig. 9 that, for $\beta = 0$ as there is no fluid helicity present in the system, additionally, the flow does not have enough stretching ability, so there is no dynamo excitation. The growth rate is also seen to be flat (blue line in Fig. 9) for higher and higher magnetic Reynolds number (R_m). The growth rate for $\beta = 0.2$ is seen to saturate over R_m , (red line in Fig. 9) though the prominent dynamo action is observed for a large range of magnetic Reynolds number (R_m) value. For higher β value, i.e., $\beta = 0.4, 0.6, 0.8$ it is noticed that, the magnetic energy growth rate increases as R_m increases, after some critical value. For all the intermediate β values, we observe significant magnetic energy growth [See Fig. 9]. We estimate the energy growth rate for the well explored $\beta = 1.0$ case, which is homologous to the conventional ABC flow. For Fig. 9 it is observed that the the growth rate of magnetic energy for $\beta = 1.0$ case increases significantly with R_m . For lower magnetic Reynolds number (R_m), there is a dip in the growth rate curve (purple line in Fig. 9), which is reported earlier as well (Galloway & Frisch 1986). It is also interesting to note that, for lower magnetic Reynolds number (R_m), the ABC dynamo model is

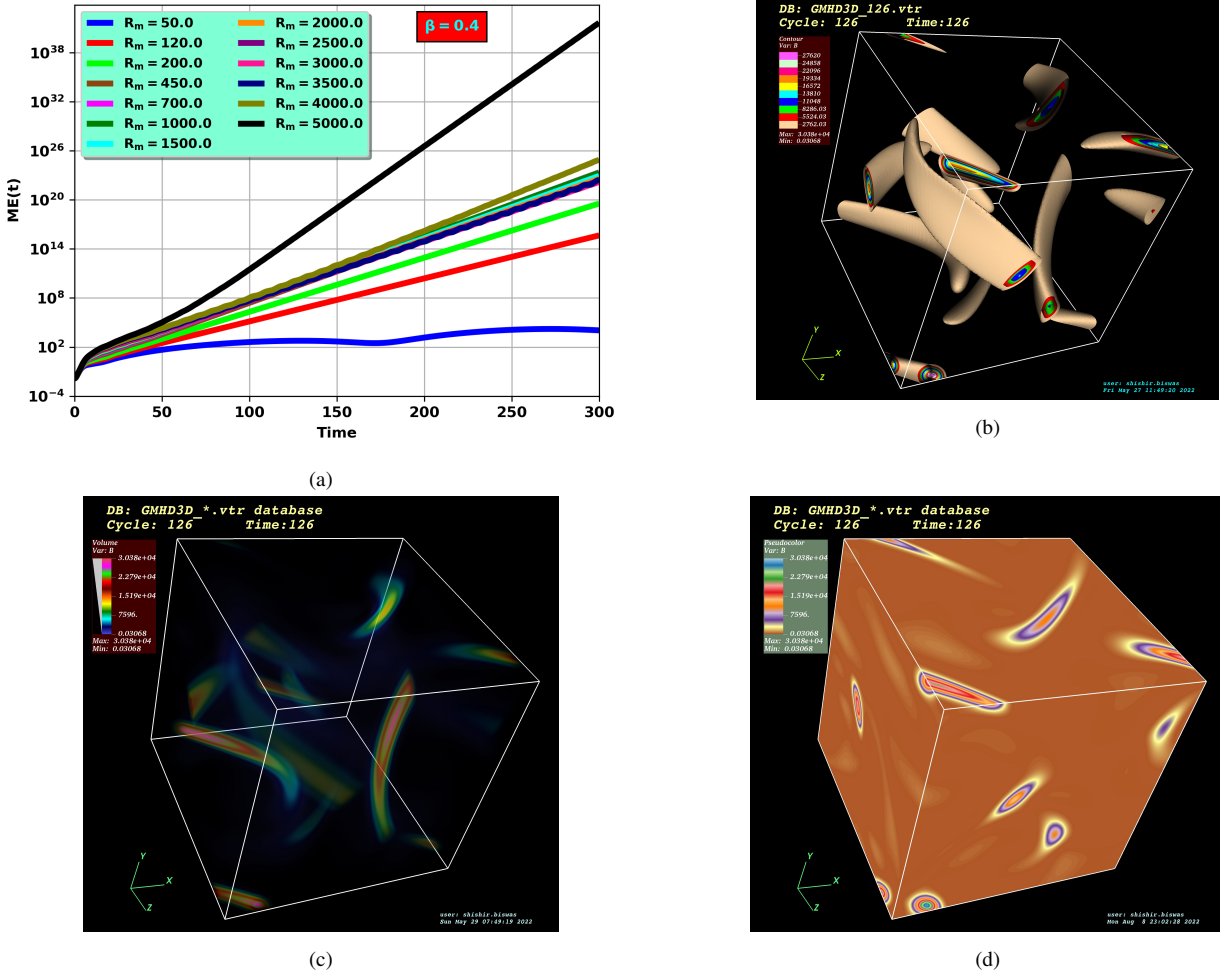


Figure 5. Kinematic fast Dynamo effect for different magnetic Reynolds number (R_m) using Yoshida-Morrison (YM) flow with $\beta = 0.4$. (a) The magnetic energy $\left(\sum \frac{B^2(x,y,z,t)}{2}\right)$ growth is observed for different R_m values. The (b) three-dimensional (3D) magnetic energy iso-surface, (c) three-dimensional (3D) volume rendering view of magnetic energy iso-surfaces and (d) three-dimensional (3D) pseudo-color view of magnetic energy iso-surfaces (for magnetic Reynolds number $R_m = 50$) is seen to be twisted “ribbon” like nature like earlier. Note that the twisting indicates the presence of helicity in the flow. Simulation details: grid resolution 256^3 , stepping time $dt = 10^{-4}$, magnitude of fluid velocity $u_0 = 1.0$, Alfvén mach number $M_A = 10.0$.

not the best dynamo model [See Fig. 9] in the sense of growth rate of magnetic energy. The magnetic energy growth rates for $\beta = 0.4$ & $\beta = 0.6$ are seen to be larger than regular ABC flow or $\beta = 1.0$, flow for lower R_m values. This observation suggests that for the YM class of flows, maximum fluid helicity does not imply the fastest dynamo action at lower R_m values.

For each of the cases mentioned above, we have determined the time-averaged magnetic energy spectrum $[\int_0^\infty B(k)dk]$. The spectra has a peak at a higher mode number, which is the hallmark of small scale dynamo (SSD), as can be seen in Fig. 10. Additionally, all of the spectra are truncated at the mode value ($k_{max} = 85$), and the peaks are in the range of $k = 15$ to 40, indicating that it is well resolved from a spectral perspective.

We have already discussed the effect of magnetic Reynolds number (R_m) on different class of YM flow at different fluid helicity. We now present our results keeping a particular R_m fixed, we study the effect of β or the effect of fluid helicity on the flow. For $R_m = 5000$, it is observed that, by varying β value from 0 to 1 magnetic energy generation rapidly enhances [See Fig. 11a]. The reason behind

this is explained via impact of fluid helicity on dynamo instability. For $\beta = 0.0$ there is no fluid helicity in the system, where as for $\beta = 1.0$ the flow is maximally helical, that generates dynamo action. The exponential energy growth for $\beta = 1.0$ flow or the ABC flow is well known so far, but here we identify a possible route that connects a non-dynamo regime ($\beta = 0.0$) to a dynamo regime ($\beta = 1.0$) via fluid helicity injection. From Fig. 11a it is verified that, the transition from non-dynamo to dynamo regime is not abrupt, but is a continuous transition that is achieved via fluid helicity injection in small steps.

To bring out the importance of our numerical findings, we examine magnetic energy growth rate evolution with R_m values 4000 and 3000 for all the class of YM flows (viz. $\beta = 0.0, 0.2, 0.4, 0.6, 0.8, 1.0$). From Fig. 11b, 11c the expected transition from non-dynamo to dynamo regime is identified via fluid helicity injection, as before. For $R_m = 2000$, a similar transition (non-dynamo to dynamo) is observed. From Fig. 11d it is observed that, there is a cross over of energy between $\beta = 0.4$ and $\beta = 0.6$ case. The energy growth is higher for a flow which has lower fluid helicity for $R_m = 2000$. To understand this “cross over” we further investigate for few lower

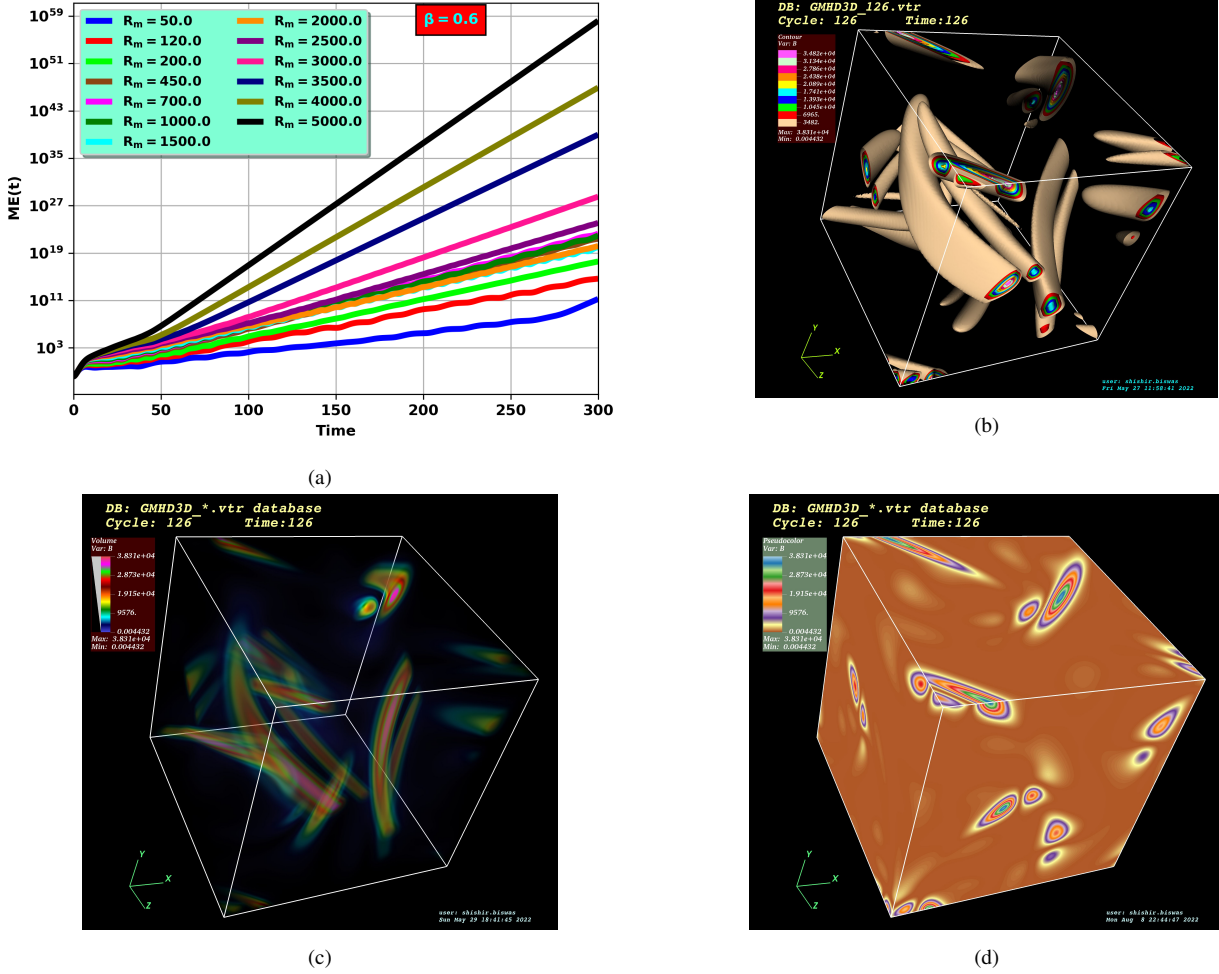


Figure 6. Kinematic fast Dynamo effect for different magnetic Reynolds number (R_m) using Yoshida-Morrison (YM) flow with $\beta = 0.6$. (a) The magnetic energy $\left(\sum \frac{B^2(x, y, z, t)}{V}\right)$ growth is observed for different R_m values. The (b) three-dimensional (3D) magnetic energy iso-surface [Supplementary movie added], (c) three-dimensional (3D) volume rendering view of magnetic energy iso-surfaces and (d) three-dimensional (3D) pseudo-color view of magnetic energy iso-surfaces (for magnetic Reynolds number $R_m = 50$) is seen to be twisted “ribbon” like nature. Due to the presence of oscillation in the magnetic energy “double ribbon” structures are observed. Simulation details: grid resolution 256^3 , stepping time $dt = 10^{-4}$, magnitude of fluid velocity $u_0 = 1.0$, Alfvén mach number $M_A = 10.0$.

magnetic Reynolds numbers (R_m). In Fig. 11e & 11f, we plot the magnetic energy growth for $R_m = 1000$ & $R_m = 450$ and observe that, the cross over is more prominent. It is also observed that, $\beta = 0.4$ & $\beta = 0.6$ shows faster dynamo action than the regular ABC flow. This is striking and from Fig. 11e & 11f one can conclude that, the YM flow with $\beta = 1.0$ or the classical ABC flow is not the best dynamo model at lower magnetic Reynolds numbers (R_m). This particular observation suggests existence of a non-monotonous relationship between flow field helicity and dynamo. It would be interesting to explore this parameter space in greater detail, in the future.

We also calculate the magnetic energy growth rate for the above discussed cases. As discussed above, a clear transition from non-dynamo regime to dynamo regime is observed in growth rate as a function of fluid helicity, for higher magnetic Reynolds number (R_m) [See Fig. 12]. From Fig. 12 it is also observed that for lower magnetic Reynolds number (R_m) the ABC model is not the best dynamo model.

It is important to indicate that, for this present study addressed so far, we have fixed $u_0 = 1.0$ and changed β , which basically changes the kinetic energy of the driving flow. We have also considered another possible approach and performed few test runs, in which we have kept the average kinetic energy ($\langle E \rangle$) constant and normalized the magnetic Reynolds number using $\langle E \rangle$. The same unambiguous shift from the non-dynamo to the dynamo regime is seen in our numerical experiment using this initial condition (not shown here). Thus, the major finding is unaffected by maintaining a constant value for the average kinetic energy.

6 SUMMARY AND CONCLUSION

In this work, we have performed direct numerical simulations of 3-dimensional magnetohydrodynamic plasmas at sufficiently high grid resolutions.

We have analyzed kinematic fast dynamo model using YM flow

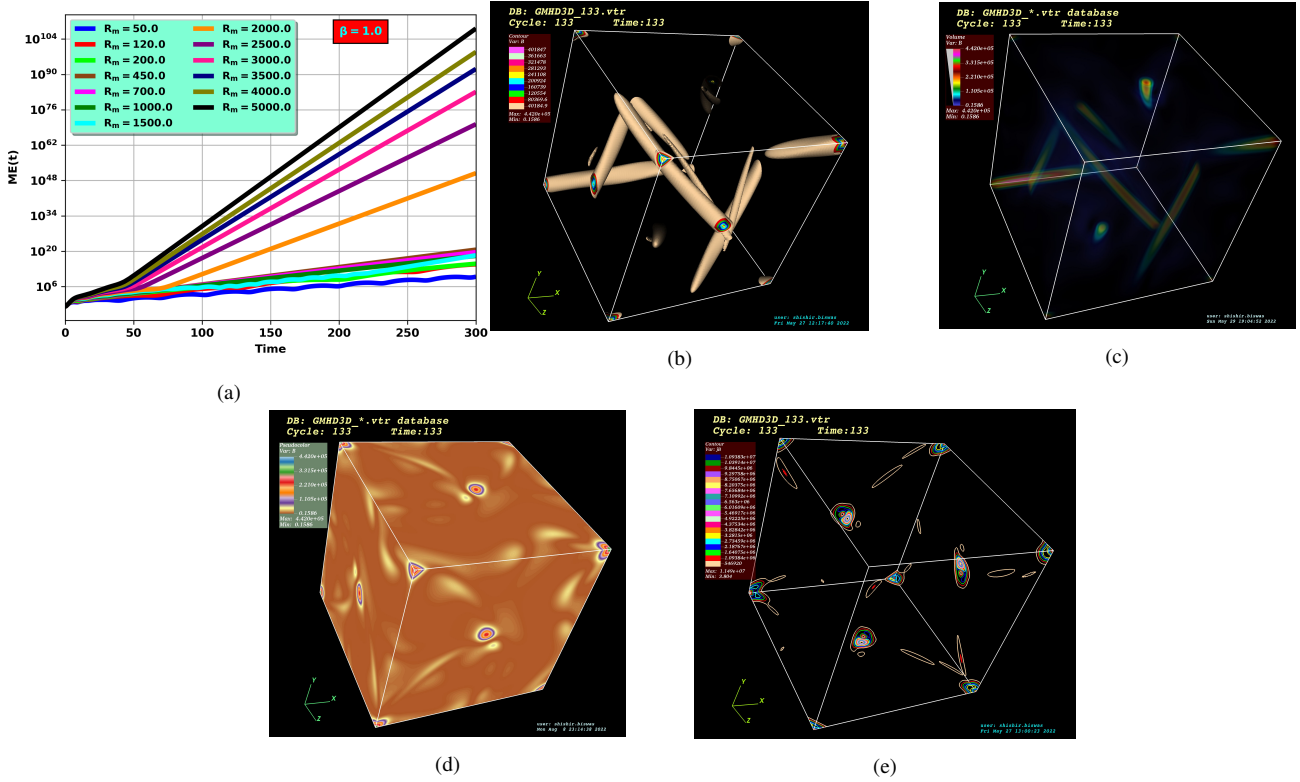


Figure 7. Kinematic fast Dynamo effect for different magnetic Reynolds number (R_m) using Yoshida-Morrison (YM) flow with $\beta = 1.0$. (a) The magnetic energy $\left(\sum \frac{B^2(x,y,z,t)}{2}\right)$ growth is observed for different R_m values. The (b) three-dimensional (3D) magnetic energy iso-surface [Supplementary movie added], (c) three-dimensional (3D) volume rendering view of magnetic energy iso-surfaces and (d) three-dimensional (3D) pseudo-color view of magnetic energy iso-surfaces (for magnetic Reynolds number $R_m = 50$) is seen to be “cigar like” in nature. (e) Strong localization of the current density is also observed. Simulation details: grid resolution 256^3 , stepping time $dt = 10^{-4}$, magnitude of fluid velocity $u_0 = 1.0$, Alfven mach number $M_A = 10.0$.

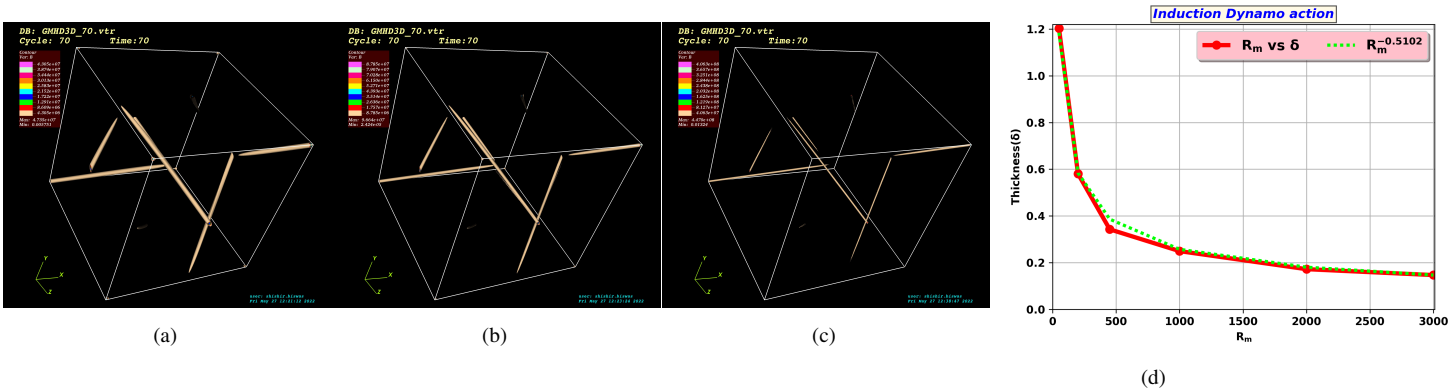


Figure 8. Three-dimensional (3D) magnetic energy iso surface for (a) $R_m = 450$, (b) $R_m = 1000$, (c) $R_m = 3000$ using Yoshida-Morrison (YM) flow with $\beta = 1.0$. (d) With the increase of R_m value the thickness of magnetic cigars (δ) are seen to be decreased with a strong scaling $\frac{1}{\sqrt{R_m}}$, which is observed earlier for ABC flow.

recently proposed by (Yoshida & Morrison 2017). An interesting and useful aspect of this flow is that, it is possible to inject finite fluid helicity $[\int_V \vec{u} \cdot (\vec{\nabla} \times \vec{u}) dV]$ in the system, by systematically varying certain physically meaningful parameter.

Our major findings are:

- Using a simple kinematic fast dynamo model, we demonstrate, a fast dynamo action primarily due to normalized fluid helicity injection. By injecting normalized fluid helicity in the system systematically, we have explored a systematic route that connects “non-dynamo” to “dynamo” regime, via direct numerical simulation.
- The study of magnetic field iso-surface is seen to exhibit untwisted ribbon like structures, when there is no helicity injection,

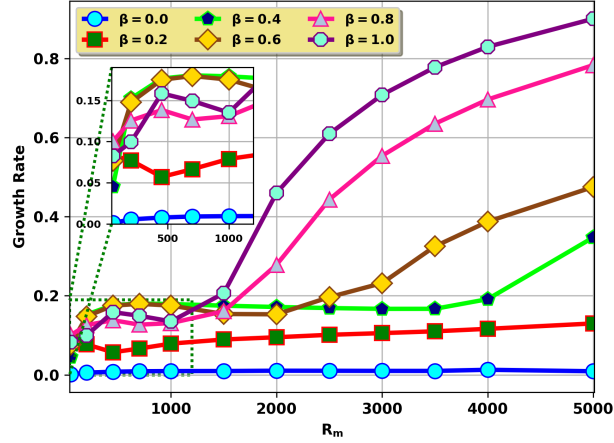


Figure 9. Magnetic energy growth rate for various class of Yoshida-Morrison (YM) flow at different magnetic Reynolds numbers (R_m). Importantly, for lower R_m it is identified that ABC flow or Yoshida-Morrison (YM) flow with $\beta = 1.0$ is not the best dynamo model.

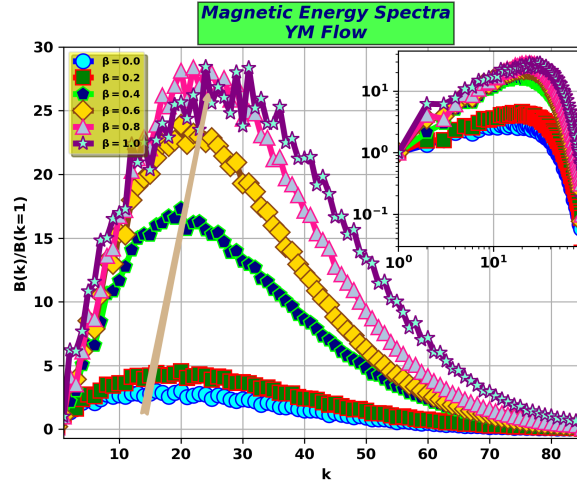


Figure 10. Time averaged (time average taken from $t = 41.0$ to 100.0) magnetic energy spectral density $B(k)$ [such that $\int B(k, t) dk$ is the total energy at time t] for different classes of Yoshida-Morrison (YM) flow at fixed magnetic Reynolds numbers ($R_m = 450.0$) are shown in linear and log-log (inset view) scales. The spatial scale spectrum clearly indicates that the dynamo is a small-scale fast dynamo. Spectra are truncated at the mode number value ($k_{max} = 85$), and the peaks are in the range of $k = 15$ to $k = 40$, indicating that it is well resolved from spectral point of view.

where as, helicity injection is shown to introduce twisting in the iso-surfaces that generates dynamo.

- We demonstrate as to, how an untwisted ribbon like non-dynamo iso-surface gets converted into cigar like fast dynamo iso-surface with the injection of fluid helicity.

- We have calculated the time-averaged magnetic energy spectrum and it is observed that, the spectra contain a discernible maxima at a higher mode number, which is the distinguishing feature of small scale dynamo (SSD).

- The conventional understanding is that a lack of reflectional symmetry (e.g., non-zero fluid helicity) is necessary for large scale dynamo action (LSD), whereas, for small scale dynamo (SSD), it is not. In our work, for the flow considered here, we demonstrate how helical structure of the flow does strongly controls the SSD growth and spectral structure. SSD. This is one of the interesting findings of the present work.

- We also identify that the most studied ABC dynamo model

is not the best suited dynamo model for lower magnetic Reynolds number problems.

To conclude, with high enough resolution and at various magnetic Reynolds number, we investigate a systematic route that connects non-dynamo to dynamo regime via fluid helicity injection. Our observation is seen to conform with the magnetic iso-surface dynamics. We have shown that, how an untwisted ribbon like non-dynamo iso-surface slowly converts to twisted ribbon like dynamo iso-surface and finally leads to cigar like fast dynamo iso-surface with injection of fluid helicity. Our work also indicates that, the fluid helicity does affect the dynamics of small-scale dynamos. We believe that, this work brings out unambiguously, the role of fluid helicity on small-scale dynamos and on the transition from “non-dynamo” to “dynamo” regime, via direct numerical simulation.

In our present work, it is demonstrated that the role of fluid helicity is the key factor to exhibit dynamo action. However, in the past,

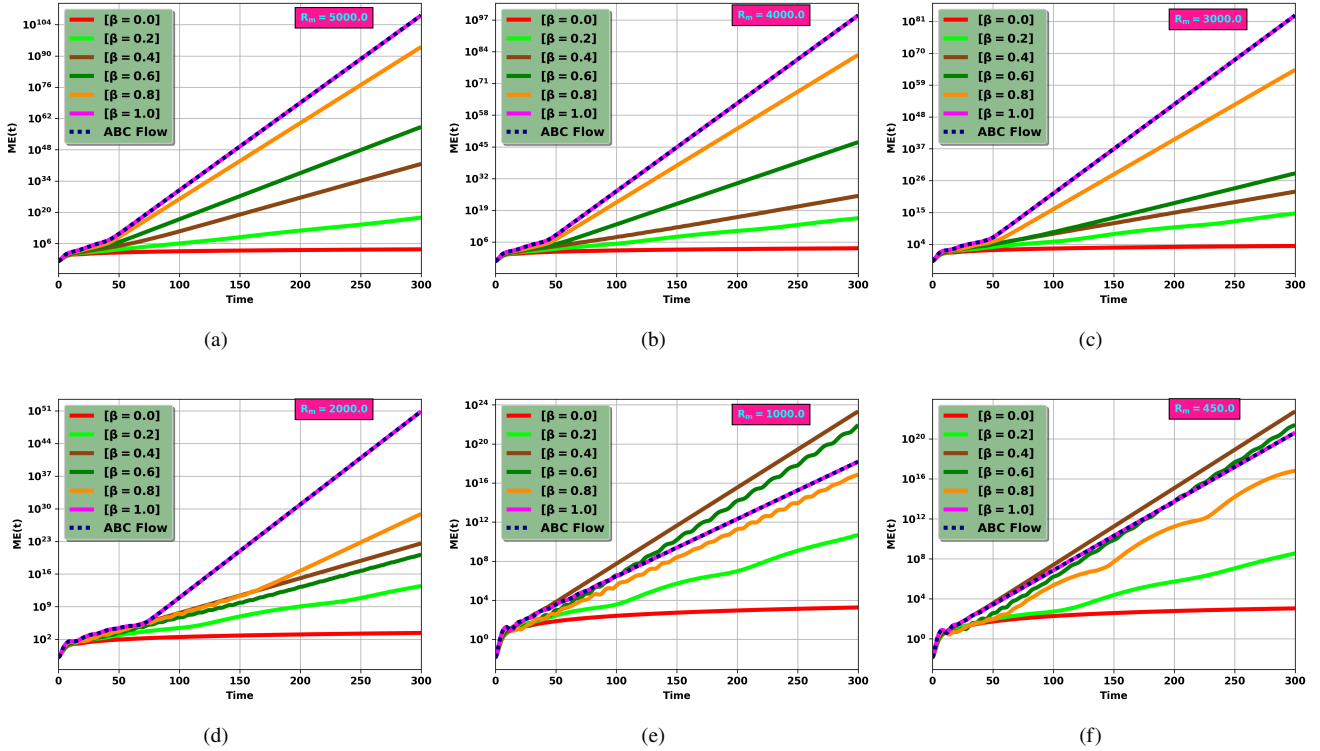


Figure 11. Exponential growth of magnetic energy for (a) $R_m = 5000$, (b) $R_m = 4000$, (c) $R_m = 3000$, (d) $R_m = 2000$, (e) $R_m = 1000$, (f) $R_m = 450$ with various class of Yoshida-Morrison (YM) flow. A clear transition from non-dynamo regime to dynamo regime is observed, at the cost of fluid helicity for higher magnetic Reynolds numbers (R_m). These figures significantly indicate the possible route that connects non-dynamo to dynamo phase.

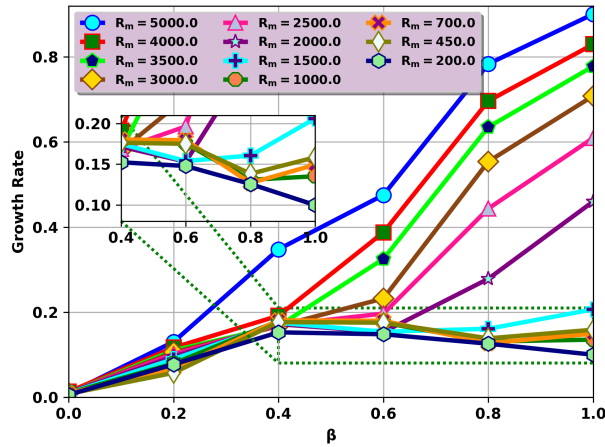


Figure 12. Magnetic energy growth rate for various class of Yoshida-Morrison (YM) flow at fixed magnetic Reynolds numbers (R_m). A notable transition from non-dynamo regime to dynamo regime is observed in growth rate, at the cost of fluid helicity injection, for higher magnetic Reynolds number (R_m).

existence of non-helical flows (i.e., flows with zero fluid helicity) to be able to generate dynamo, in Kinematic Fast and Saturation (with magnetic feedback) dynamo models (Galloway & Proctor 1992; Sur & Brandenburg 2009), wherein cross-helicity (also called Yoshizawa effect) is shown to play a crucial role. However the investigation of the role of cross-helicity (also called Yoshizawa effect) on YM flow and others, in the context of various dynamo action is beyond the scope of the present work and will be addressed in future communication. The effect of fluid helicity injection in the context of recurrence

(Mukherjee et al. 2019) and quasi-recurrence (Biswas et al. 2022b) phenomenon is also an interesting study to investigate out, that will also be reported soon. The role of hydro-dynamically unstable shear flow (Biswas & Ganesh 2022) at the largest scale is interesting to investigate in this context. We hope to attempt this problem in the near future.

7 ACKNOWLEDGMENTS

The simulations and visualizations presented here are performed on GPU nodes and visualization nodes of Antya cluster at the Institute for Plasma Research (IPR), INDIA. One of the author S.B is thankful to Dr. Rupak Mukherjee at Central University of Sikkim (CUS), Gangtok, Sikkim, India for providing an initial version of *GMHD3D* code. S.B thanks N. Vydyanathan, Bengaluru and B. K. Sharma at NVIDIA, Bengaluru, India, for extending their help with basic GPU methods. S.B is grateful to Mr. Soumen De Karmakar at IPR, India for many helpful discussions regarding GPUs, and HPC support team of IPR for extending their help related to ANTAYA cluster. The authors would also like to thank Dr. Jugal Chowdhury from IPR for careful reviewing the manuscript and for his valuable suggestions.

8 DATA AVAILABILITY

The data underlying this article will be shared on reasonable request to the corresponding author.

9 CONFLICT OF INTEREST

The authors have no conflicts to disclose.

10 SUPPORTING INFORMATION

Supplementary movies:

- [YM_beta_0p0_B_Field_IsoB.mp4](#)
- [YM_beta_0p2_B_Field_IsoB.mp4](#)
- [YM_beta_0p6_B_Field_IsoB.mp4](#)
- [YM_beta_1p0_B_Field_IsoB.mp4](#)

are added.

REFERENCES

- Alexakis A., 2011, *Phys. Rev. E*, 83, 036301
- Archontis, V. Dorch, S. B. F. Nordlund, Å. 2003, *A&A*, 397, 393
- Arnold V., Korkina E., 1983, *Matem. Mekh.*, 3, 43
- Beresnyak A., 2019, *Living Reviews in Computational Astrophysics*, 5, 1
- Biskamp D., 2003, *MagnetoHydrodynamic turbulence*. Cambridge University Press
- Biswas S., Ganesh R., 2022, *Physics of Fluids*, 34, 065101
- Biswas S., Ganesh R., et al. 2022a, GPU Technology Conference 2022, <https://www.nvidia.com/en-us/on-demand/session/gtcspring22-s41199/>
- Biswas S., Ganesh R., Mukherjee R., Sen A., 2022b, “Three Dimensional MagnetoHydroDynamics of EPI Two Dimensional Flows: Quasi-recurrence and nonlinear Alfvén wave oscillations”, Manuscript under preparation
- Bouya I., Dormy E., 2013, *Physics of Fluids*, 25, 037103
- Brachet M. E., Meneguzzi M., Politano H., Sulem P. L., 1988, *Journal of Fluid Mechanics*, 194, 333–349
- Cattaneo F., Kim E.-j., Proctor M., Tao L., 1995, *Phys. Rev. Lett.*, 75, 1522
- Cattaneo F., Hughes D. W., Kim E.-j., 1996, *Phys. Rev. Lett.*, 76, 2057
- Childress S., Gilbert A. D., 1995, *Stretch, twist, fold: the fast dynamo*. Vol. 37, Springer Science & Business Media
- Choudhuri A. R., 1990, *The Astrophysical Journal*, 355, 733
- Courvoisier A., Hughes D. W., Tobias S. M., 2006, *Phys. Rev. Lett.*, 96, 034503
- Dombre T., Frisch U., Greene J. M., Hénon M., Mehr A., Soward A. M., 1986, *Journal of Fluid Mechanics*, 167, 353–391

- Dorch S. B. F., 2000, *Physica Scripta*, 61, 717
- Galanti B., Sulem P. L., Pouquet A., 1992, *Geophysical & Astrophysical Fluid Dynamics*, 66, 183
- Galloway D., Frisch U., 1984, *Geophysical & Astrophysical Fluid Dynamics*, 29, 13
- Galloway D., Frisch U., 1986, *Geophysical & Astrophysical Fluid Dynamics*, 36, 53
- Galloway D. J., Proctor M. R., 1992, *Nature*, 356, 691
- Gholami A., Hill J., Malhotra D., Biro G., 2016, <http://arxiv.org/abs/1506.07933>
- Hughes D. W., Cattaneo F., Jin Kim E., 1996, *Physics Letters A*, 223, 167
- Kitware 2022, Paraview, <https://www.paraview.org/>
- Kraichnan R. H., 1965, *The Physics of Fluids*, 8, 1385
- LLNL 2020, VisIt, <https://wci.llnl.gov/simulation/computer-codes/visit/releases/release-notes-3.1.2>
- Mukherjee R., June, 2019, “Turbulence, Flows and Magnetic Field Generation in Plasmas using a MagnetoHydrodynamic Model”: HBNI Phd Thesis
- Mukherjee R., Ganesh R., Sen A., 2019, *Physics of Plasmas*, 26, 022101
- Parker E., 1979, *Cosmical Magnetic Fields*, Clarendon
- Patterson G. S., Orszag S. A., 1971, *The Physics of Fluids*, 14, 2538
- Paulo-herrera 2021, PyEVTk, <https://github.com/paulo-herrera/PyEVTk>
- Rädler K.-H., Brandenburg A., 2003, *Phys. Rev. E*, 67, 026401
- Rincon F., 2019, *Journal of Plasma Physics*, 85, 205850401
- Schekochihin A. A., 2022, *Journal of Plasma Physics*, 88, 155880501
- Squire J., Bhattacharjee A., 2014a, *Phys. Rev. Lett.*, 113, 025006
- Squire J., Bhattacharjee A., 2014b, *The Astrophysical Journal*, 797, 67
- Squire J., Bhattacharjee A., 2015, *The Astrophysical Journal*, 813, 52
- Sur S., Brandenburg A., 2009, *Monthly Notices of the Royal Astronomical Society*, 399, 273
- Tobias S. M., Cattaneo F., 2013, *Nature*, 497, 463
- Vainshtein S. I., Zel’dovich Y. B., 1972, *Soviet Physics Uspekhi*, 15, 159
- Yoshida Z., Morrison P. J., 2017, *Phys. Rev. Lett.*, 119, 244501

APPENDIX A: FLUID HELICITY CALCULATION FOR YOSHIDA-MORRISON (YM) FLOW

Fluid helicity is defined as,

$$H_f = \int_V \vec{u} \cdot (\vec{\nabla} \times \vec{u}) dV.$$

Here,

$$\vec{u} = \hat{i} (\alpha u_0 [B \sin(k_0 y) - C \cos(k_0 z)]) + \hat{j} (\beta u_0 [C \sin(k_0 z) - A \cos(k_0 x)]) + \hat{k} (u_0 [\alpha A \sin(k_0 x) - \beta B \cos(k_0 y)]).$$

Taking curl and putting the real constant value, $\alpha = A = B = C = 1.0$, $k_0 = 1.0$, we get,

$$\vec{\nabla} \times \vec{u} = \hat{i} (\beta u_0 [\sin y - \cos z]) + \hat{j} (u_0 [\cos x - \sin z]) + \hat{k} (u_0 [\beta \sin x - \cos y])$$

Taking $\vec{u} \cdot$ on both side,

$$\vec{u} \cdot \vec{\nabla} \times \vec{u} = (u_0 [\sin y - \cos z]) (\beta u_0 [\sin y - \cos z]) + (\beta u_0 [\sin z - \cos x]) (u_0 [\cos x - \sin z]) \\ + (u_0 [\sin x - \beta \cos y]) (u_0 [\beta \sin x - \cos y]).$$

or,

$$\vec{u} \cdot \vec{\nabla} \times \vec{u} = \beta u_0^2 [(\sin y - \cos z)^2] - \beta u_0^2 [(\cos x - \sin z)^2] + u_0^2 [(\sin x - \beta \cos y)(\beta \sin x - \cos y)]$$

or,

$$\vec{u} \cdot \vec{\nabla} \times \vec{u} = \beta u_0^2 [(\sin^2 y + \cos^2 z - 2 \sin y \cos z)] - \beta u_0^2 [(\cos^2 x + \sin^2 z - 2 \cos x \sin z)] \\ + u_0^2 [(\beta \sin^2 x - \sin x \cos y - \beta^2 \sin x \cos y + \beta \cos^2 y)]$$

Integrating over total volume,

$$\int_V \vec{u} \cdot (\vec{\nabla} \times \vec{u}) dV = \beta u_0^2 \left[\left(\int_0^{2\pi} \int_0^{2\pi} \int_0^{2\pi} \sin^2 y dx dy dz + \int_0^{2\pi} \int_0^{2\pi} \int_0^{2\pi} \cos^2 z dx dy dz - \int_0^{2\pi} \int_0^{2\pi} \int_0^{2\pi} 2 \sin y \cos z dx dy dz \right) \right. \\ \left. - \beta u_0^2 \left[\left(\int_0^{2\pi} \int_0^{2\pi} \int_0^{2\pi} \cos^2 x dx dy dz + \int_0^{2\pi} \int_0^{2\pi} \int_0^{2\pi} \sin^2 z dx dy dz - \int_0^{2\pi} \int_0^{2\pi} \int_0^{2\pi} 2 \cos x \sin z dx dy dz \right) \right] \right. \\ \left. + \beta u_0^2 \left[\left(\int_0^{2\pi} \int_0^{2\pi} \int_0^{2\pi} \sin^2 x dx dy dz \right) - u_0^2 \left[\int_0^{2\pi} \int_0^{2\pi} \int_0^{2\pi} \sin x \cos y dx dy dz \right] \right. \right. \\ \left. \left. - \beta^2 u_0^2 \left[\int_0^{2\pi} \int_0^{2\pi} \int_0^{2\pi} \sin x \cos y dx dy dz \right] + \beta u_0^2 \left[\int_0^{2\pi} \int_0^{2\pi} \int_0^{2\pi} \cos^2 y dx dy dz \right] \right] \right]$$

Finally after simplification one obtains,

$$\int_V \vec{u} \cdot (\vec{\nabla} \times \vec{u}) dV = 8\pi^3 \beta u_0^2$$

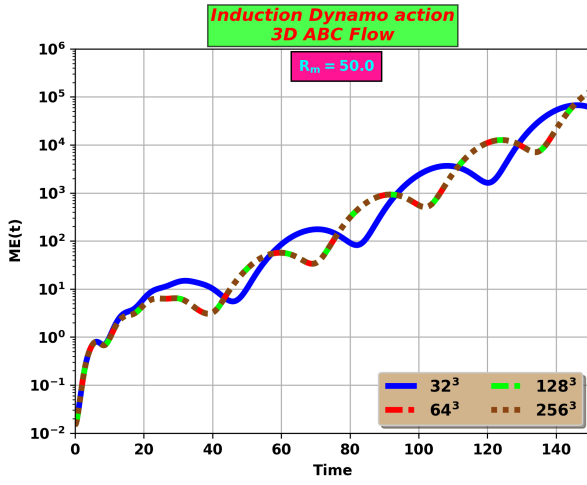
Considering velocity to be normalized,

$$H_f = \beta$$

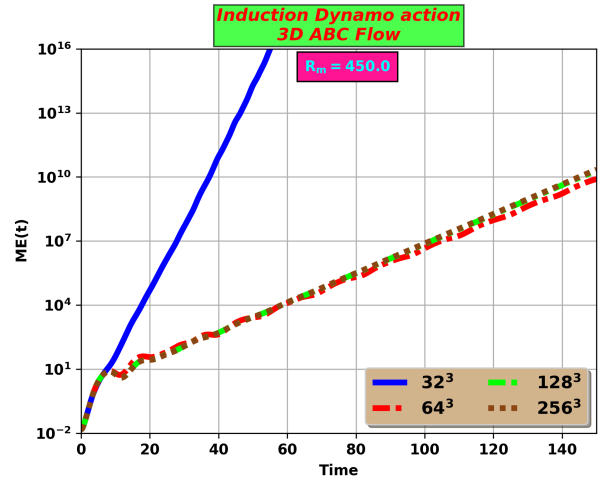
So normalized fluid helicity for YM flow depends upon constant β value of the flow.

APPENDIX B: GRID SIZE SCALING STUDY FOR ABC FLOW

Grid size scaling study have been performed using Arnold-Beltrami-Childress (ABC) flow [Eq. 3] at different magnetic Reynolds numbers. It is seen that 256^3 grid resolution is more than enough for this problem [See Fig. B1a, B1b].



(a)



(b)

Figure B1. Fast Dynamo effect following Galloway et al. (Galloway & Frisch 1984) using Arnold-Beltrami-Childress (ABC) flow for magnetic Reynolds numbers (a) $R_m = 50.0$ (b) $R_m = 450.0$ at different grid resolutions.